Inorganic Chemistry
Article

Inorg. Chem. **2009**, *48*, 6471–6479 **6471**
DOI: 10.1021/ic900420m

Biomineralization of Uniform Gallium Oxide Rods with Cellular Compatibility

Danhong Yan,[†] Guangfu Yin,[†] Zhongbing Huang,*[,†] Xiaoming Liao,[†] Yunqing Kang,[†] Yadong Yao,[†] Baoqing Hao,*[,‡] Jianwen Gu,*[,§] and Dong Han[∥]

[†]*College of Materials Science and Engineering, Sichuan University, Chengdu, 610065, China,* [‡]*College of Life Science & Technology, Southwest University for Nationalities, China,* [§]*The Military General Hospital of Chengdu PLA, China, and* [∥]*Zhengzhou Research Institute, Aluminum Corporation of China Limited, China*

Received March 3, 2009

Monodispersed single crystalline α-GaOOH rods coated by silk fibroin (SF) have been prepared via a facile biomineralization process in the template of SF peptide. The carbon-coated α-Ga_2O_3 and β-Ga_2O_3 rods are obtained by thermal treatment of the α-GaOOH rods at 600 and 800 °C, respectively. In vitro cytotoxicity studies of these gallium oxide rods showed no significant effect leading to restraint of cell proliferation of L929, Hela, and HaCat cells in less than 0.1 mg/mL prepared rods. On the basis of their excellent luminescence emission properties and cellular compatibilities, possible applications for bio-optoelectronic devices can be envisioned.

Introduction

Gallium oxide, with a wide band gap of 4.9 eV at room temperature, is one of the most important semiconductors. Its unique conduction[1] and luminescence[2] properties make it a host candidate for gas sensors,[3,4] catalysis,[5,6] and optoelectronic devices.[7] Recently, many high-temperature methods such as physical evaporation,[8] arc discharge,[9] metal organic chemical vapor deposition,[10] catalytic-assisted processes,[11] the laser ablation method,[12] thermal annealing of milled GaN powders,[13] and plasma immersion ion implantation[14] have been developed for the synthesis of β-Ga_2O_3. Among the diverse synthesis procedures of crystalline Ga_2O_3, the most convenient and frequently applied route is via thermal treatment of the precursor, gallium oxyhydroxide (α-GaOOH), which can be readily synthesized by wet chemical methods. Zhang et al. reported the formation of GaOOH by a solvothermal process at 180 °C and the formation of β-Ga_2O_3 after annealing the samples at 900 °C.[15] Qian et al. prepared monodispersed single crystalline α-GaOOH spindles via a wet chemical route at 60 °C.[16] Ristić et al. obtained nanosized α-GaOOH particles by the addition of a TMAH solution to the solution of gallium(III)-isopropoxide dissolved in 2-propanol.[17] Patra et al. fabricated submicrometer-sized GaOOH rods by refluxing an aqueous solution of $Ga(NO_3)_3$ and NH_4OH in a microwave oven.[18] However, there are some disadvantages in these methods, such as the requirements of complicated apparatuses, too high of an annealing temperature, harsh conditions or surfactants, and the utilization of alkalis. These techniques could result in the contamination of the final product, which makes them hard to apply in a biomaterial field.

*To whom correspondence should be addressed. Tel.: 86-28-85413003 (Z.H.), 86-28-86714164 (B.H.), 86-28-86570362, 86570361 (J.G.). Fax: 86-28-85413003 (Z.H.). E-mail: zbhuang@iccas.ac.cn (Z.H.), bqhao@mail.sc.cninfo.net (B.H.), gujianwen5000@yahoo.com.cn (J.G.).

(1) Hajnal, Z. J.; MirÓ, J.; Kiss, G.; Réti, F.; Deák, P.; Herndon, R. C.; Kuperberg, J. M. *J. Appl. Phys.* **1999**, *86*, 3792.
(2) Wu, X. C.; Song, W. H.; Huang, W. D.; Pu, M. H.; Zhao, B.; Sun, Y. P.; Du, J. J. *Chem. Phys. Lett.* **2000**, *328*, 5.
(3) Ogita, M.; Higo, K.; Nakanishi, Y.; Hatanaka, Y. *Appl. Surf. Sci.* **2001**, *175*, 721.
(4) Weh, T.; Frank, J.; Fleischer, M.; Meixner, H. *Sens. Actuators B: Chem.* **2001**, *78*, 202.
(5) Nakagawa, K.; Kajita, C.; Okumura, K.; Ikenaga, N.-O.; Nishitani-Gamo, M.; Ando, T.; Kobayashi, T.; Suzuki, T. *J. Catal.* **2001**, *203*, 87.
(6) Petre, A. L.; Auroux, A.; Gelin, P.; Caldararu, M.; Ionescu, N. I. *Thermochim. Acta.* **2001**, *379*, 177.
(7) Xiao, T.; Kitai, A. H.; Liu, G.; Nakua, A. *J. Appl. Phys. Lett.* **1998**, *72*, 3356.
(8) Yang, Z. X.; Jin, Y. S. *Appl. Surf. Sci.* **2007**, *253*, 3393.
(9) Choi, Y. C.; Kim, W. S.; Park, Y. S.; Lee, S. M.; Bae, D. J.; Lee, Y. H.; Park, G. S.; Choi, W. B.; Lee, N. S.; Kim, J. M. *Adv. Mater.* **2000**, *12*, 746.
(10) Kyoko, H.; Masahiro, F.; Hirokazu, S.; Shigemi, K.; Toetsu, S.; Masaoki, O.; Masanori, M.; Yoshio, B. *J. Alloys Compd.* **2005**, *390*, 261.
(11) Liang, C. H.; Mebg, G. W.; Wang, G. Z.; Wang, Y. W.; Zhang, L. D.; Zhang, S. Y. *Appl. Phys. Lett.* **2001**, *78*, 3202.
(12) Raina, G.; Kulkarni, G. U.; Rao, C. N. R. *Mater. Res. Bull.* **2004**, *39*, 1271.
(13) Lee, J. -S.; Park, K.; Nahm, S.; Kim, S.-W.; Kim, S. *J. Cryst. Growth* **2002**, *244*, 287.
(14) Lo, K. C.; Ho, H. P.; Fu, K. Y.; Chu, P. K. *Surf. Coat. Technol.* **2007**, *201*, 6804.
(15) Zhang, J.; Liu, Z.; Lin, C.; Lin, J. *J. Cryst. Growth* **2005**, *280*, 99.
(16) Qian, H. S.; Gunawan, P.; Zhang, Y. X.; Lin, G. F.; Zheng, J. W.; Xu, R. *Cryst. Growth Des.* **2008**, *8*, 1282.
(17) Ristić, M.; Popović, S.; Musić, S. *Mater. Lett.* **2005**, *59*, 1227.
(18) Patra, C. R.; Mastai, Y.; Gedanken, A. *J. Nanopart. Res.* **2004**, *6*, 509.

Published on Web 06/18/2009

Moreover, toxicity studies in rats have shown that gallium oxide could produce toxicity to organs, tissues, and the immune system.[19−21] Therefore, it is of great significance to produce nontoxic and good biocompatible gallium oxide for possible applications in the biomedicine field on the basis of its unique semiconduction and luminescence properties.[22]

In recent years, a facile room-temperature aqueous mineralization process has been developed, in which mild reaction conditions under normal atmospheric pressure are required, the natural biomineralization process conditions are mimicked,[23] and biotemplates are used as the structure-directing agent to control the nucleation and yield a unique crystal structure. For example, peptides with an affinity for metals and semiconductors, such as gold, silver, silica, zinc sulfide, and cadmium selenide, can be used to synthesize crystalline nano- to micrometer-sized materials.[24−28] Kisailus et al. developed an enzyme catalytic process using the artificial protein filaments as both the template and the catalyst for the hydrolysis and polycondensation of $Ga(NO_3)_3$ to yield either α-GaOOH attached to the filament.[29] However, these artificial protein filaments were expensive and hard to obtain. As known to all, silk fibroin (SF) is one of the most extensively applied biomaterials, and it can be hydrolyzed into a peptide providing nucleophilic hydroxyl of amino acids, which would be very important in the nucleation of the biomineralization process.

In this paper, single-crystalline α-GaOOH rods with a coating layer of peptide could be successfully fabricated through a facile biomineralization process in the template of a SF peptide at room temperature. These SF peptides could not only promote the hydrolysis and polycondensation of the gallium precursor to yield α-GaOOH at room temperature but also direct its crystalline growth. Furthermore, single crystalline α-Ga_2O_3 and β-Ga_2O_3 rods could also be selectively obtained via a thermal decomposition method using α-GaOOH. In vitro cytotoxicity studies of these prepared gallium oxide rods with SF polypeptide or carbonized coating layers present good cellular compatibility at a concentration of less than 0.1 mg/mL, indicating that the prepared gallium oxide rods have a possible application in bio-optoelectronic devices in the future.

Experimental Procedures

Bombyx mori SF was boiled for 30 min in a 0.3% Na_2CO_3 solution to degum the gluelike sericin coating, then was dried and hydrolyzed in 6 M HCl at 80 °C for 24 h. The pH value of the SF hydrolysate solution was adjusted to 7 and dialyzed with distilled water for about 24 h at 4 °C.

In a typical synthesis, 0.352 g of gallium chloride ($GaCl_3$, anhydrous, 99.99%) was dissolved in 20 mL of deionized water to form a clear solution in a bottle (50 mL in total volume) under magnetic stirring. Then, 2 mL of a SF peptide solution (0.1 mg/mL) was mixed into this solution. An ammonia solution was added drop by drop until a pH of 10 was reached. Then, the bottle was capped and incubated in the dark at room temperature. When a white precipitate was observed, it was centrifuged and rinsed with deionized water and ethanol in sequence three times and finally dried at 60 °C for 24 h. As-prepared α-GaOOH powders were calcined in a muffle furnaceto (SX2.5-12, Zhongshan Instrument Plant of Xiangtan) to produce α-Ga_2O_3 and β-Ga_2O_3 at 600 and 800 °C for 30 min, respectively.

The shapes and crystalline structures of synthesized crystals were studied by transmission electron microscopy (TEM; JEOL-200, 160 kV; JEOL-2000, high resolution (HR) TEM, operating at 200 kV, Japan) and accompanying selected area electron diffraction (SAED) and scaning electron microscopy (SEM; JEOL-5900LV, 20 kV). The SAED patterns were obtained at a camera distance of 60 cm. In the preparation of TEM specimens, 1.0 mL of the crystal suspension was dropped on the Formvar/carbon-coated copper grid and dried in the air. An energy-dispersive X-ray spectroscope (EDX) attached to the HRTEM was used to analyze the composition of samples. The X-ray diffraction (XRD) pattern was recorded on a Philips X'Pert MDP diffractometer with Cu Kα radiation. Fourier transform infrared (FT-IR) spectra were recorded by an IRPrestige-21 spectrometer. The photoluminescence (PL) measurements were performed at room temperature using a Xe laser (300 nm in wavelength) as the excitation light source on a fluorescence spectrophotometer (F-7000, HITACHI, Japan). The laser pulse frequency was 15 Hz, with a pulse duration of 800 ps at an average energy of 50 mW. Synchronization of differential thermal analysis (SDTA) and thermogravimetry (TG) were carried out with a TG/SDTA851^e analyzer from METTLER-TOLEDO Co. of Switzerland. Approximately 10 mg of the powder was placed into an alumina vessel and heated at a rate of 5 °C/min up to 1000 °C in the air.

The L929 fibroblast cell line, Human Hela cell line, and keratinocyte HaCat cell line were gifted by the College of Life and Science, Sichuan University, China. Cell lines were cultured in Dulbecco's modified Eagle's medium (DMEM, Gibco) supplemented with 10% fetal bovine serum (Gibco, BRL), 1 mM L-glutamina, penicillin (20 000 U/mL), and streptomycin (20 000 μg/mL), under a CO_2 (5%) atmosphere and at 37 °C.

The cell viability was chosen as a cytotoxicity parameter and determined by the MTT assay, which was applied to evaluate the effect of gallium oxide particles on L929, Hela, and HaCat cell viability by measuring the uptake and reduction of tetrazolium salt to an insoluble formazan dye by cellular microsomal enzymes. A total of 200 μL of cells was added to 96-well plates (BD Biosciences) at an initial concentration of approximately 2×10^4 cells/well. When the cells reached confluence, 50 μL of gallium oxide suspensions with different concentrations were added and then were cultured at 37 °C. Control cells were incubated in a gallium oxide-free medium. After the addition of gallium oxide particles for 24 h, cells were visualized using an inverted microscope produced by Zeiss, model Axiovert 35, equipped with a digital microscopy camera processed with the Viewfinder

(19) Akiyo, T.; Akira, H.; Miyuki, H.; Noburu, I. *Appl. Organomet. Chem.* **1990**, *4*, 231.
(20) Webb, D. R.; Wilson, S. E.; Carter, D. E. *Toxicol. Appl. Pharmacol.* **1986**, *82*, 405.
(21) Wolff, R. K.; Henderson, R. F.; Eidson, A. F.; Pickrell, J. A.; Rothenberg, S. J.; Hahn, F. F. *J. Appl. Toxicol.* **1988**, *8*, 191.
(22) Kisailus, D.; Truong, Q.; Amemiya, Y.; Weaver, J. C.; Morse, D. E. *Proc. Natl. Acad. Sci. U.S.A.* **2006**, *103*, 5652.
(23) Xia, Y.; Yang, P.; Sun, Y.; Wu, Y.; Mayers, B.; Gates, B.; Yin, Y.; Kim, F.; Yan, H. *Adv. Mater.* **2003**, *15*, 353.
(24) Brown, S.; Sarikaya, M.; Johnson, E. *J. Mol. Biol.* **2000**, *299*, 725.
(25) Naik, R. R.; Stringer, S. J.; Agarwal, G.; Jones, S.; Stone, M. O. *Nat. Mater.* **2002**, *1*, 169.
(26) Naik, R. R.; Brott, L. L.; Clarson, S. J.; Stone, M. O. *J. Nanosci. Nanotechnol.* **2002**, *2*, 95.
(27) Mao, C.; Flynn, C. E.; Hayhurst, A.; Sweeney, R.; Qi, J.; Georgiou, G.; Iverson, B.; Belcher, A. M. *Proc. Natl. Acad. Sci. U.S.A.* **2003**, *100*, 6946.
(28) Mao, C.; Solis, D. J.; Reiss, B. D.; Kottmann, S. T.; Sweeney, R. Y.; Hayhurst, A.; Georgiou, G.; Iverson, B.; Belcher, A. M. *Science* **2004**, *303*, 213.
(29) Kisailus, D.; Choi, J. H.; Weaver, J. C.; Yang, W. J.; Morse, D. E. *Adv. Mater.* **2005**, *17*, 314.

program. At the end of the designed incubation time, 20 μL of a 5 mg/mL MTT-PBS solution was added to each well and was incubated further at 37 °C for 4 h. Then, 150 μL of dimethyl sulfoxide was added to each well after the incubating solution was removed. Finally, the plates were incubated for 30 min at room temperature. The absorbance of solubilized formazan at 490 nm was measured with a Microplate Reader 3550 (Bio-Rad). The cell viability was calculated by the following formula: cell viability (%) = optical density (OD) of the treated cells/OD of the nontreated cells. All of the experiments were performed in triplicate.

Data are expressed as means ± standard deviations of a representative of three similar experiments carried out in triplicate. Statistical analysis was performed using the Statistical Package for the Social Sciences version 13.0 software. Statistical comparisons were made by analysis of variance. Either Scheffé or Games-Howell tests were used for post hoc evaluations of differences between groups. In all statistical evaluations, $p < 0.05$ was considered as statistically significant.

Results and Discussion

Figure 1 shows the XRD patterns of the samples obtained by the process of biomineralization at room temperature after 4 weeks and the oxide products obtained by calcinations at 600 and 800 °C. Figure 1a can be readily indexed to a pure orthorhombic phase of α-GaOOH with lattice constants $a = 4.555$ Å, $b = 9.801$ Å, and $c = 2.974$ Å (JCPDS 54-0910). No characteristic peaks from other phases were observed, indicating that the gallium precursor was completely polycondensed and crystallized into α-GaOOH capped with the peptide assemblies by the process of biomineralization. Figure 1b shows that pure-phase α-Ga_2O_3 could be obtained by calcination of α-GaOOH at 600 °C. All of the peaks can be indexed to a pure rhombohedral phase of α-Ga_2O_3 with lattice constants $a = 4.979$ Å, $b = 4.979$ Å, and $c = 13.429$ Å (JCPDS 06-0503). Due to there being 2 equiv of GaOOH to $Ga_2O_3 \cdot H_2O$, all of the GaOOH powders could be removed their crystal waters and changed into Ga_2O_3. When the thermal annealing temperature is increased to 800 °C, the monoclinic phase of β-Ga_2O_3 with lattice constants $a = 12.227$ Å, $b = 3.039$ Å, and $c = 5.808$ Å (JCPDS 41-1103) is obtained (shown in Figure 1c), because the phase transition temperature from α-Ga_2O_3 to β-Ga_2O_3 is above 750 °C.[30] According to the Scherrer formula, the evaluated average crystallite sizes of α-GaOOH, α-Ga_2O_3, and β-Ga_2O_3 rods are 62.7, 88.9, and 105.4 nm, respectively, indicating that crystal fusion happened during the calcinations.

To understand the growth process, the mineralization growth of α-GaOOH was monitored with SEM at different growth stages. After 6 h, lots of gel-like aggregation and nanoparticles with an average diameter of 100 nm (marked by a white arrow in Figure 2a) were observed. It is known that the fresh precipitates exist as an amorphous gallium hydroxide $Ga(OH)_3$, which is transformed to crystalline α-GaOOH during aging in hot solution.[31] Although lots of amorphous $Ga(OH)_3$ appeared, some α-GaOOH particles with a rodlike shape (marked by a black arrow) were observed, see Figure 2a. During the mineralization, the amount of $Ga(OH)_3$ gel gradually decreased because some gels were polycondensed and crystallized to form the smaller α-GaOOH,

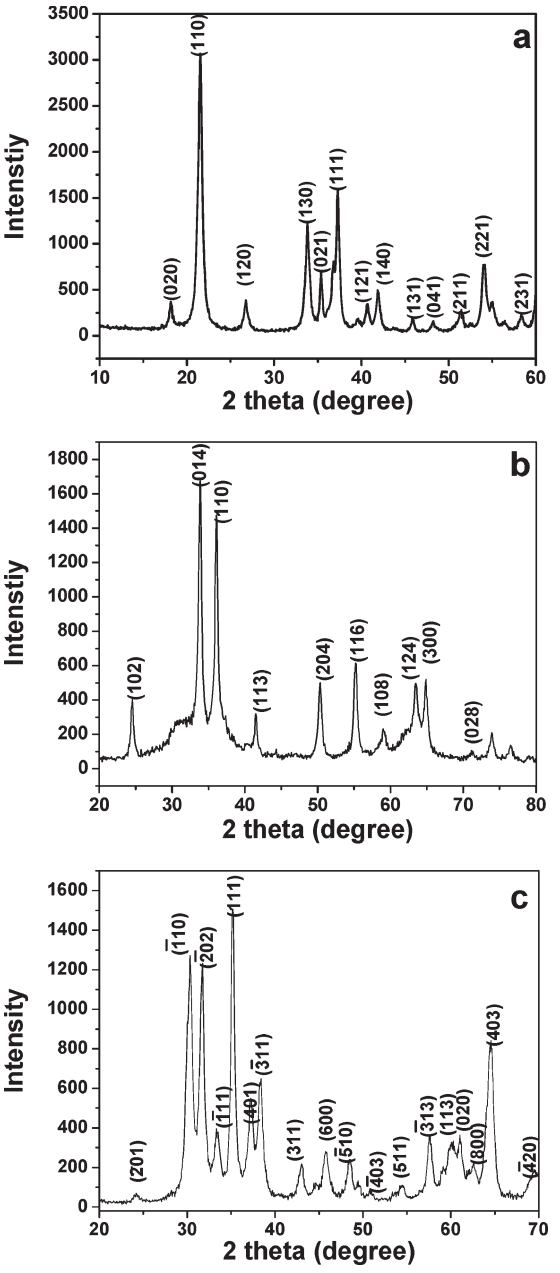

Figure 1. XRD patterns of the obtained samples: (a) α-GaOOH, (b) α-Ga_2O_3, and (c) β-Ga_2O_3.

followed by the growth of rodlike particles. After mineralization for 12 h, a number of rodlike α-GaOOH's with an average length of 800 nm were formed (shown in Figure 2b), although a little amorphous $Ga(OH)_3$ was also observed. However, $Ga(OH)_3$ gels were not observed in the 1-day-old sample shown in Figure 2c, and the size of rodlike α-GaOOH was larger than that at 12 h, suggesting that most of the $Ga(OH)_3$ gels have been polycondensed and crystallized into larger α-GaOOH rods in the catalysis of the SF peptide templates. After 2 weeks of biomineralization at room temperature, α-GaOOH rods with a diameter of 250 nm and a length of 1.2 μm were fabricated (shown in Figure 2d). The morphology of α-GaOOH obtained after 28 days was more obvious (shown in Figure 2e). The results indicated that the yield of α-GaOOH was increased with the increase of biomineralization time. These rods were composed of many

(30) Roy, R.; Hill, V. G.; Obson, E. F. *J. Am. Chem. Soc.* **1952**, *74*, 719.
(31) Sato, T.; Nakamura, T. J. *Chem. Technol. Biotechnol.* **1982**, *32*, 469.

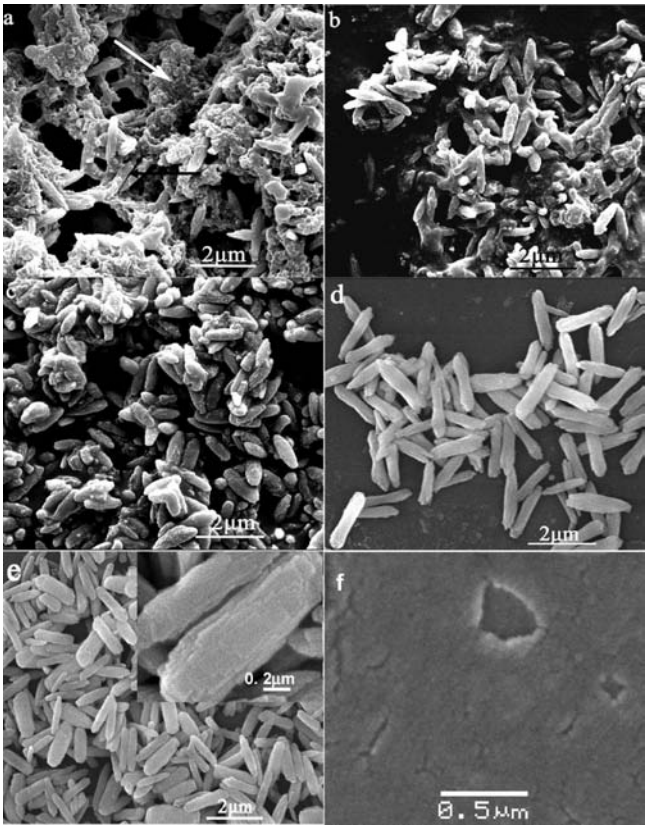

Figure 2. SEM images of samples obtained from biomineralization with SF peptide at room temperature at pH 10 after (a) 6 h, (b) 12 h, (c) 1 days, (d) 14 days, (e) 28 days, and (f) 1 day without SF peptide.

well-aligned nanoplatelets with a thickness of less than 100 nm, exhibiting that a layered structure and the edges of the individual nanoplatelets could be easily distinguished on their surfaces (inset of Figure 2e). However, the result in Figure 2f shows that there were not α-GaOOH rods in the sample without the SF peptide templates.

Obviously, SF peptide could be utilized as a template and structure-directing agent for the polycondensation and crystallization of $Ga(OH)_3$ to α-GaOOH in the process of biomineralization. Silk is spun by *B. mori* and mainly consists of two major proteins: SF, the major structural protein, and sericin, the gluelike protein.[32] SF, which can be removed from the outer sericin with anhydrous sodium carbonate solution, is one of the most extensively studied biomaterials due to its good biodegradability and biocompatibility.[33] SFs are composed of two polypeptide chains linked by a disulfide bridge. The larger heavy chain (391 kDa) is comprised of 12 low-complexity "crystalline" domains made up of Gly-X repeating units and covering 94% of the sequence; X is Ala in 64%, Ser in 22%, Tyr in 10%, Val in 3%, and Thr in 1.3% of the repeating units.[34,35] The detailed amino acid composition of silk fibroin of *B. mori* is presented in Table 1. As we known from Table 1, SF includes an abundance of hydrophilic and

Table 1. Amino Acid Composition of Silk Fibroin of *Bombyx mori*[34,35]

amino acid	Asp	Thr	Ser	Glu	Gly	Ala	Val	Tyr
percentage (mol %)	4.43	1.61	12.51	1.13	39.42	34.92	1.11	0.41
amino acid	Ile	Leu	Phe	Lys	His	Arg	Pro	
percentage (mol %)	0.07	0.18	0.08	0.79	0.17	0.90	0.26	

hydrophobic amino acid residues. The polymer region including hydrophobic amino acid residues (Ala and Gly) could not form a β-sheet and deposit, while hydrophilic amino acid residues in the polymer region including Tyr and Ser present good solubility in water. Thus, lots of micellelike conglomeration could be formed in the solution due to SF's specific hydrophobic/hydrophilic structure, which would be in favor of biomineralization.[23] Previous reports have revealed that the locations and functionality of the active site residues facilitating the biomineralization process contain the catalytic triad (serine, histidine, and asparagine residues).[36] Site-directed mutagenesis studies have confirmed that interaction between the essential serine and histidine side chains at the active site increase the nucleophilicity of the serine oxygen, which could promote the attack of Ga ions and subsequent hydrolysis from $Ga(OH)_3$.[37] As displayed in Table 1, SF peptides possess lots of serine as well as a few histidine and asparagine residues. These residues could randomly form catalytic triads, which could provide some nucleophilic hydroxyls and a nucleophilicity-enhancing hydrogen-bonding imidazole nitrogen. In the micellelike conglomeration of SF peptides, hydrogen bonding can occur between the hydroxyl group of serine and the imidazole residue of adjacent histidine; thereby, the nucleophilicity of the serine oxygen could be increased. The enhanced nucleophilicity of the hydroxyl side chains could facilitate an attack of Ga ions to form a transitory Ga−O bond and the deprotonation and subsequent hydrolysis of $Ga(OH)_3$.[38,39]

Figure 3 shows SEM images of products prepared by the thermal treatment of as-prepared α-GaOOH (28-day-old sample) at 600 and 800 °C for 30 min. The oxide products retain the features of the pristine rodlike α-GaOOH well in terms of good dispersion, size uniformity, and layered nanostructure.

For a better understanding of their crystal structures, HRTEM observation was carried out on individual rods. The insert in Figure 4a displays the image of an α-GaOOH rod obtained by biomineralization after 4 weeks. The HRTEM image shows that the interplanar spacing is 2.97 Å, corresponding to the (002) crystal plane of GaOOH. The SAED pattern in Figure 4a reveals a single-crystalline structure of the sample, and the diffraction spots can be indexed to a pure orthorhombic structure of α-GaOOH, suggesting a good quality of crystalline structure during the room-temperature biomineralization. These are in accordance with the XRD results. The crystal orientations of the nanoplatelets along the length, width, and thickness are

(32) Gage, L. P.; Manning, R. F. *J. Biol. Chem.* **1980**, *255*, 9444.
(33) Oguz, B.; Ozge, M.; Yarkin, O.; Aysegul, B. *Eur. J. Pharm. Biopharm.* **2005**, *60*, 373.
(34) Chen, X.; Shao, Z.; Marinkovic, N. S.; Miller, L. M.; Zhou, P.; Chance, M. R. *Biophys. Chem.* **2001**, *89*, 25.
(35) Tanaka, K.; Kajiyama, N.; Ishikura, K.; Waga, S.; Kikuchi, A.; Ohtomo, K.; Takagi, T.; Mizuno, S. *Protein Struct. Mol. Enzym.* **1999**, *1432*, 92.
(36) Mita, K.; Ichimura, S.; Zama, M.; James, T. C. *J. Mol. Biol.* **1988**, *203*, 917.
(37) Dodson, G.; Wlodawer, A. *Trends Biochem. Sci.* **1998**, *23*, 347.
(38) Baes, C. F.; Mesmer, R. E. *The Hydrolysis of Cations*; Wiley: New York, 1976.
(39) Henry, M.; Jolivet, J. P.; Livage, J. *Chem. Spectrosc. Appl. Sol-Gel Glasses* **1992**, *77*, 153.

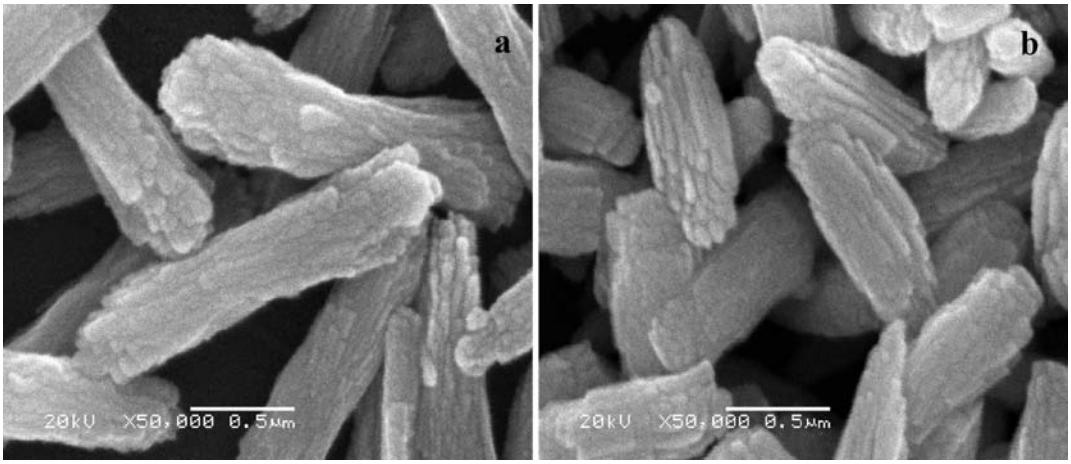

Figure 3. SEM images of products prepared by the calcination of a biomineralized sample at (a) 600 °C and (b) 800 °C for 30 min.

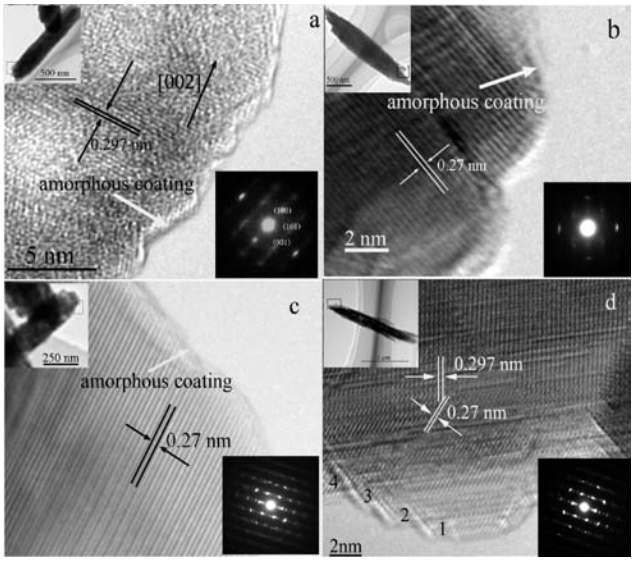

Figure 4. HRTEM images of the rectangle region (inset in the upper-left-hand corner) and the corresponding SAED pattern (insert in lower-right-hand corner): (a) α-GaOOH, (b) α-Ga_2O_3, (c, d) β-Ga_2O_3. All of the samples are coated with amorphous layers (marked with white arrows).

determined to be in the [001], [100], and [101] directions (*c* axis), which corresponds with the characteristics of the α-GaOOH crystal structure. The octahedral interstices in the α-GaOOH structure are occupied by Ga ions, while the oxygen-hydroxyl sheets form a hexagonal close-packed array.[40,41] In general, a crystal face with more closely packed ions has a lower density of unsaturated bonds and a lower specific surface free energy.[42] On the basis of the gallium ion density difference, the crystal plane with the lowest and highest surface energy is {010} and {001}, respectively. Thus, α-GaOOH grows preferentially along the longitudinal *c* axis, and the largest facet of an equilibrium shape of a diaspore-like crystal belongs to {010} faces. In addition, the α-GaOOH is covered with a thin layer of amorphous coating (marked with the white arrow in Figure 4a), indicating that the SF peptides have incorporated onto α-GaOOH during biomineralization. Figure 4b shows the HRTEM image and corresponding SAED pattern of α-Ga_2O_3. The measured distance between parallel lattice planes is 0.270 nm, corresponding to a *d* spacing of the $(10\bar{1}0)$ planes. Amorphous coating (marked with a white arrow) results from the carbonized SF peptide on the surface of α-Ga_2O_3. Figure 4c shows a perfect lattice with a closest interplanar interval of 0.297 nm. The corresponding SAED pattern reveals a single-crystalline structure of the samples, and the diffraction spots can be indexed to a pure monoclinic phase of β-Ga_2O_3, which is in accordance with the XRD result. Carbonized compounds (marked with white arrows in Figure 4c) coated in the surface of β-Ga_2O_3 could also be distinguished from HRTEM. Figure 4d obviously shows the typical layered feature of β-Ga_2O_3, and Figures 1−4 point out the typical layers of ultrathin nanoplatelets overlapping. Consistent with SEM results, the rodlike particles are comprised of layer-by-layer assembled nanoplatelets.

Figure 5 shows the FT-IR transmission spectra of α-GaOOH, α-Ga_2O_3, and β-Ga_2O_3. As shown in Figure 5a, the IR bands at 3403 and 3240 cm^{-1} and the shoulder at 2980 cm^{-1} are well-visible at high wave numbers. The band at 3403 cm^{-1} represents the −OH stretching vibrations of H_2O molecules in the particles, whereas the bands at 3240 and 2980 are due to stretching vibrations of structural −OH groups. The characteristic IR bands, corresponding to δ(OH) deformation vibrations, are located at 1014 and 954 cm^{-1}, and their first overtones could be located at 2002 cm^{-1} and 1950 cm^{-1}. The IR band at 688 cm^{-1} can be assigned to γ(OH) deformation vibrations, whereas the bands at 640 cm^{-1} and 483 cm^{-1} are due to Ga−O vibrations.[43] Peaks at about 1633 and 1390 cm^{-1} are assigned to the vibration of amide I and amide II, respectively, suggesting that there are SF peptides on the surface of GaOOH rods. Figure 5b and c show FT-IR transmission spectra of α-Ga_2O_3 rods and β-Ga_2O_3 rods. The absorption peaks of α-Ga_2O_3 are located at 671 and 462 cm^{-1} (shown in Figure 5b), and the absorption peaks of β-Ga_2O_3 are 577 and 509 cm^{-1} (shown in Figure 5c). The altered peak locations obviously result from the different scale of Ga−O bonds in different gallium oxide rods. In addition, the location of a hydroxy stretch (corresponds to two absorption peaks at 3437 and 1635 cm^{-1}) is observed. The appearance of a hydroxy stretch should result from H_2O

(40) Hill, R. J. *Phys. Chem. Miner.* **1979**, *5*, 179.
(41) Klug, A.; Farkas, L. *Phys. Chem. Miner.* **1981**, *7*, 138.
(42) Markov, I. V. *Crystal Growth for Beginners*, 2nd ed.; World Scientific Publishing: Singapore, 2003
(43) Xiao, H. D.; Ma, H. L.; Xue, C. S.; Hu, W. R.; Ma, J.; Zong, F. J.; Zhang, X. J.; Ji, F. *Mater. Lett.* **2004**, *58*, 3925.

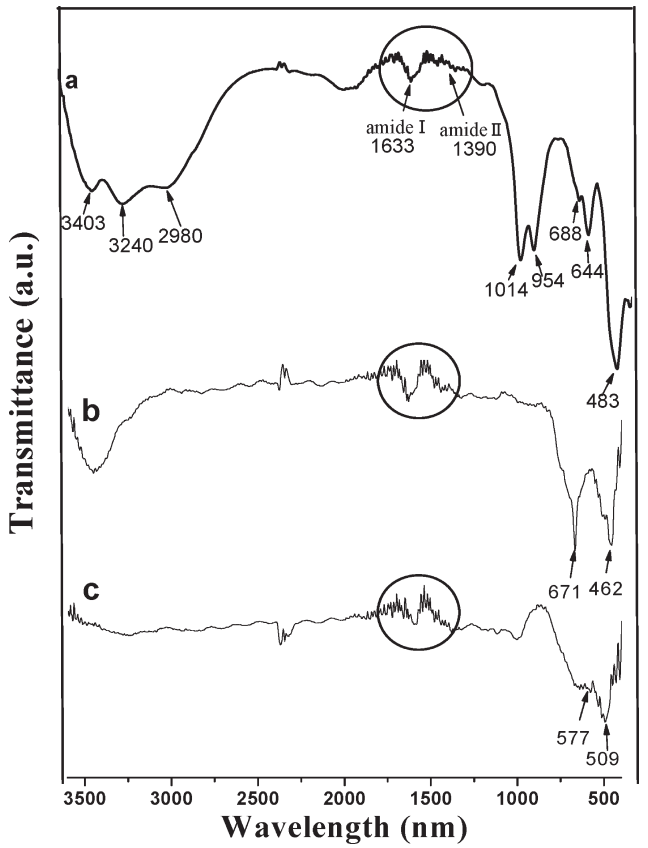

Figure 5. FT-IR transmission spectra of (a) α-GaOOH, (b) α-Ga_2O_3, and (c) β-Ga_2O_3.

being absorbed in powders. It was interesting that the amide I and amide II located at 1633 and 1390 cm^{-1} could still be detected in the Ga_2O_3 powders after calcination at 600 or even 800 °C, indicating that there is a carbonized portion of SF peptide still coated on the surface of Ga_2O_3 powder after calcination for 30 min.

For further understanding of the composition of the samples, the EDX technique was performed to analyze the different atom percents of as-prepared samples. Atoms Ga, C, and O could be easily distinguished, as shown in Figure 6a, suggesting that carbon compounds have incorporated into the GaOOH sample. Obviously, these carbon compounds result from the SF peptide during biomineralization, which was in accordance with IR and HRTEM results. Atom C still existed in α-Ga_2O_3 and β-Ga_2O_3 samples after calcination at 600 and 800 °C (shown in Figure 6b and c), respectively, indicating that the SF peptide was carbonized and remained on the surface of Ga_2O_3. Such a carbonized substance provided a special "coating layer", which is in favor of cellular compatibility.[44,45] The lower ratio of O/Ga in GaOOH, α-Ga_2O_3, and β-Ga_2O_3 (listed in Table 2) displayed that there were a great number of oxygen vacancies in these three gallium oxide crystalline structures, especially in and on the edges and surfaces of nanoplatelets, which are inevitable in the biomineralization or calcination process. Atom Cu in

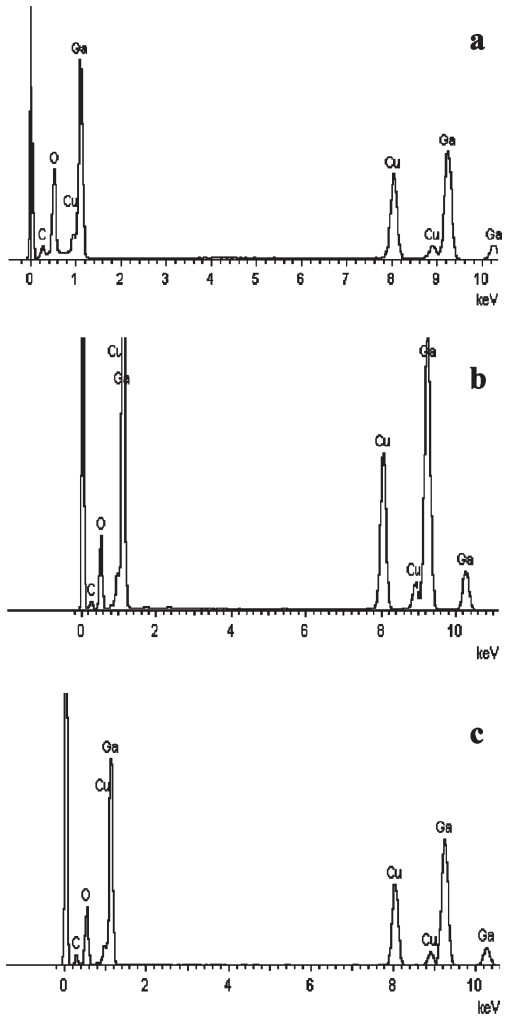

Figure 6. EDX spectra of (a) α-GaOOH, (b) α-Ga_2O_3, and (c) β-Ga_2O_3.

Table 2. Elements Composition of α-GaOOH, α-Ga_2O_3, and β-Ga_2O_3

	percent of atoms		
element	α-GaOOH	α-Ga_2O_3	β-Ga_2O_3
C K	3.52	1.24	3.36
O K	18.36	8.00	12.52
Cu K	29.00	27.10	27.34
Ga K	49.11	63.67	56.78
total		100.00	

Figure 6 originated from the Cu webs for supporting TEM specimens.

Figure 7 displays the room-temperature PL spectra of α-GaOOH, α-Ga_2O_3, and β-Ga_2O_3 rods under an excitation wavelength of 300 nm. Luminescence bands centered at around 389 and 466 nm are observed. The blue emission bands centered at 389 nm are assigned to the recombination a self-trapped excitation. The blue emission centered at 466 nm originates from the recombination of an electron on a donor formed by an oxygen vacancy and a hole on an acceptor by either a gallium vacancy or gallium−oxygen vacancy pairs.[46−48] In our

(44) Lam, C. W.; James, J. T.; McCluskey, R.; Hunter, R. L. *Toxicol. Sci.* **2004**, *77*, 126.
(45) Jin, M.; Masako, Y.; Takeshi, A.; Yoshimi, K.; Sumio, I. *ACS Nano* **2008**, *2*, 213
(46) Harwig, T.; Kellendonk, F. *J. Solid State Chem.* **1978**, *24*, 255.
(47) Binet, L.; Gourier, D. *J. Phys. Chem. Solids* **1998**, *59*, 1241.
(48) Liang, C. H.; Meng, G. W.; Wang, G. Z.; Zhang, L. D.; Zhang, S. Y. *Appl. Phys. Lett.* **2001**, *78*, 3202.

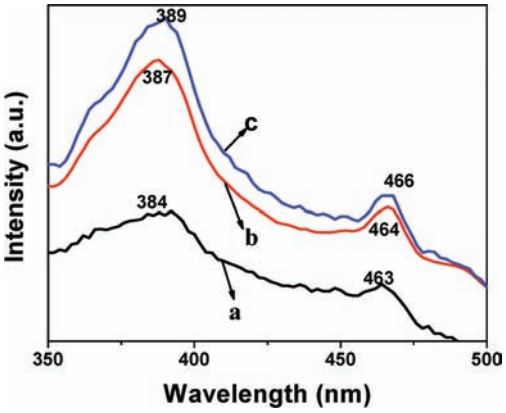

Figure 7. Room-temperature PL spectra of (a) α-GaOOH, (b) α-Ga_2O_3, and (c) β-Ga_2O_3.

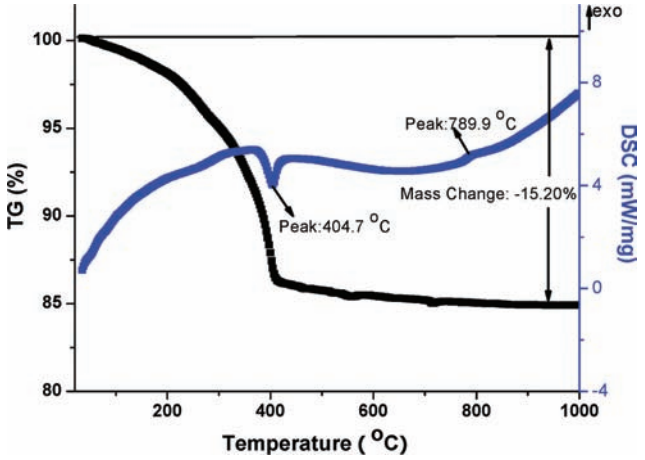

Figure 8. TG-DSC curve of the α-GaOOH in the temperature range of 20−1000 °C.

experiments, various defects, oxygen vacancies, and gallium−oxygen vacancy pair creation are inevitable in the biomineralization of α-GaOOH rods in the template of a SF peptide, which would result in a weaker PL intensity of α-GaOOH. A higher calcination temperature could reduce the intensity of the emission from the defects (centered at 466 nm) and enhance the intensity of the emission from the intrinsic phase (centered at 389 nm), indicating that the crystallinity of Ga_2O_3 is increased, which is in accordance with the HRTEM results. Since the preparation process is simple, it is believed that the method can be used to synthesize other excellent optical metal and semiconductor oxide micrometer rods.

Figure 8 shows the thermogravimetry−differential scanning calorimetry (TG-DSC) curve of the α-GaOOH rods in the temperature range of 20−1000 °C. The sharper endothermic peak at around 404.7 °C should indicate the dehydration of α-GaOOH and the formation of α-Ga_2O_3. The exothermic peak at around 789.9 °C in the DSC curve shows the conversion of α-Ga_2O_3 into β-Ga_2O_3 crystals.[49,50] In general, the transformation of GaOOH into Ga_2O_3 upon thermal dehydration ($GaOOH = 1/2Ga_2O_3 + 1/2H_2O$) would cause about a 9% loss in weight. However, the weight loss reached a high value of 15.20%, indicating that more than

(49) Huang, C. C.; Yeh, C. S.; Ho, C. J. *J. Phys. Chem., B* **2004**, *108*, 4940.
(50) Tas, A. C.; Majewski, P. J.; Aldinger, F. *J. Am. Ceram. Soc.* **2002**, *85*, 1421.

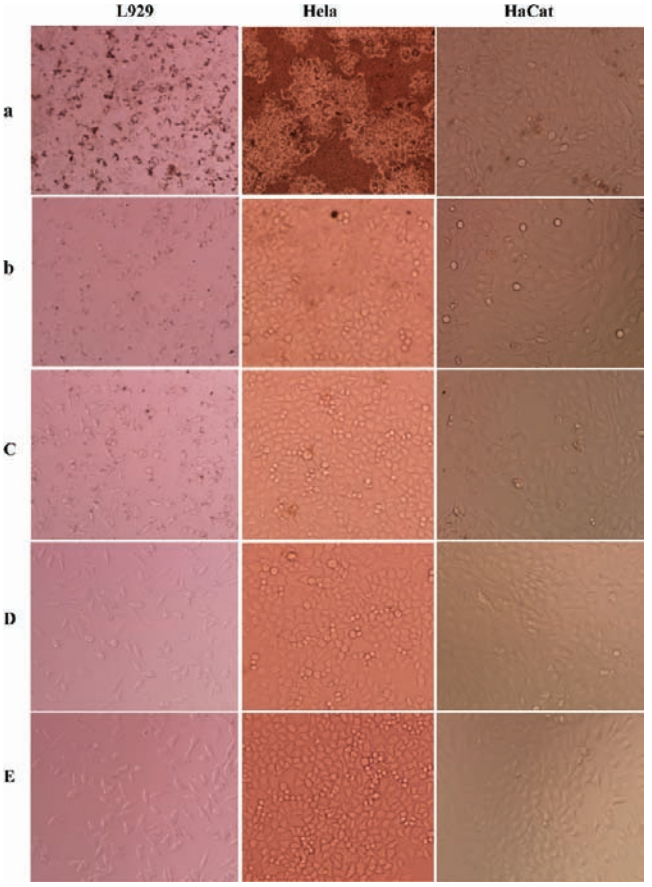

Figure 9. Photomicrographs of cells after treatment with different concentrations of β-Ga_2O_3 for 24 h: (A) 0.5 mg/mL, (B) 0.1 mg/mL, (C) 0.02 mg/mL, (D) 0.004 mg/mL, and (E) 0 mg/mL.

6.20% was the result of a loss of SF peptide during the calcination. Because labile short peptides and amino acids were calcined into CO_2 and H_2O, and then volatilized without remains, longer and more solid peptides were calcined and carbonized on the surface of gallium oxide. Furthermore, as shown in the TG curve, continued weight loss even over 1000 °C suggested that the calcination of the SF peptide was still in process and there still existed the carbonized substance on the Ga_2O_3 samples after calcination at 800 °C, which was in accordance with IR and HRTEM results.

In vitro cellular compatibility investigations were performed to assess the cytotoxicity of gallium oxide particles upon L929, Hela, and HaCat cells. Figure 9 shows photomicrographs of cells after being treated for 24 h with a β-Ga_2O_3 suspension with concentrations of 0.5 mg/mL, 0.1 mg/mL, 0.02 mg/mL, and 0.004 mg/mL. The treatment of β-Ga_2O_3 of a high concentration (0.5 mg/mL) produced a great deal of extra material deposited on the cells and "mechanically" induced extra stress to damage the cells. In the treatment of 0.1−0.004 mg/mL β-Ga_2O_3 particles, cell changes were not remarkable in the morphology or even the density of cells. Only some cells became rounded and were destroyed in the visual field. The number of cells was not reduced significantly in comparison with the control cell culture. These results reveal that the treatment of 0.1−0.004 mg/mL β-Ga_2O_3 particles produced different effects from that of 0.5 mg/mL β-Ga_2O_3 particles.

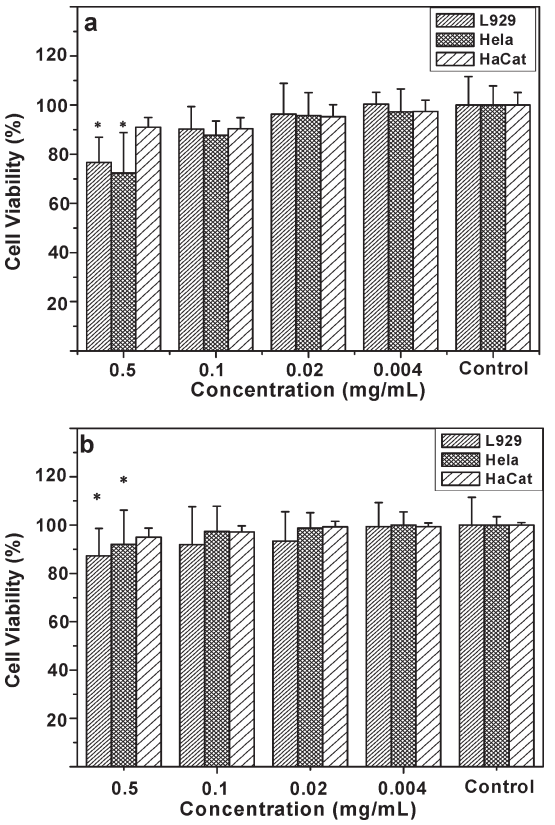

Figure 10. Cell viability of L929, Hela, and HaCat cells incubated with concentrations of 0.5, 0.1, 0.02, and 0.004 mg/mL of (a) GaOOH and (b) β-Ga_2O_3 suspensions at 37 °C for 24 h, respectively. Error bars indicate standard deviation. An asterisk (*) represents a significant difference.

In order to quantify the cytotoxicity of gallium oxide particles upon L929, Hela, and HaCat cell cultures, an MTT assay was performed to determine the surviving fraction in the presence of different concentrations of gallium oxide suspensions. Figure 10 indicates that a 0.5 mg/mL particle suspension showed a significant effect ($p < 0.05$) of restraining cell proliferation of L929 and Hela cells; however, no significant effect emerged upon human keratode HaCat cells. A 0.1 mg/mL suspension could slightly restrain cell proliferation of L929, Hela, and HaCat cells, but these effects were not significant enough for any conclusion to be drawn. In the treatments of low concentrations (20 and 4 μg/mL), all of the experimental cells showed good resistance to the cytotoxicity of gallium oxide. The cell viabilities of those groups were close to 100% survival, which was in accordance with the results of optical micrographs. In our work, seemingly, human keratode HaCat cells had better resistance to cytotoxicity of the particles. This could be explained by a functional adaptation of HaCat cells to the environment permanently exposed to the oxidation/reduction processes. Because of these frequent oxidation/reduction processes, we could suggest that HaCat possesses a large amount of antioxidative enzymes able to scavenge the reactive oxygen species (ROS). As known to all, several nanomaterials, including quantum dots and metal oxide NP,[51,52] could induce the generation of ROS, resulting in modification and damage of the cellular proteins, DNA, and lipids, which can lead to cell death.[53] Gallium oxide, in traditional ideas, is a heavy metal oxide and has been proved to produce toxicity to the lungs, immune system, and hematopoietic systems.[20−22] However, in our study, low toxicity gallium oxide rods are fabricated, and no significant cytotoxicity is showed toward L929, Hela, and HaCat cells in concentrations of less than 0.1 mg/mL; namely, their good cellular compatibilities appear. Obviously, the SF peptide plays an important role in the cellualr compatibility. SF is well-suited for cell culture purposes. Both Chiarini et al.[54] and Minoura et al.[55] reported that SF coated membranes permitted greater adherence and consequently greater proliferation of fibroblasts in comparison to noncoated membranes. In this case, the coated SF peptide in GaOOH could be absorbed by cells and promote proliferation. IR and EDX analysis showed that SF peptide was carbonized and remained on the surface of Ga_2O_3. Carbon materials are regarded to be nonirritant and nontoxic through extensive in vitro and in vivo toxicological assessments.[44,45] These carbonization structures on the surface of Ga_2O_3 possess similar properties to those of carbon materials, which can avoid ROS generation from the surface of the Ga_2O_3 rods and prevent the nanostructure surface of Ga_2O_3 from the directly contacting the cell membrane. In that case, Ga_2O_3 rods would not damage cellular biolipid film and easily enter into cell without damaging cellular proteins, DNA, and lipids. Thus, these carbonization structures lead to excellent cellular compatibility of Ga_2O_3 particles.

It should be noted that, when an α-GaOOH rod with SF peptides contacts cells, its cellular compatibility is difficult to maintain for a long time because SF peptides could be absorbed by cells through metabolism over time. Thus, it is necessary that α-GaOOH rods prepared by biomineralization be calcined and transformed into Ga_2O_3 rods with carbon coating layers, which could lead to good cellular compatibility of the Ga_2O_3 rod. In addition, their good photoluminescence properties are improved after the calcination

Conclusions

Monodispersed single crystalline α-GaOOH rods have been successfully synthesized through a facile biomineralization process in the catalysis of SF peptides at room temperature. The biomineralization process involves the hydrolysis and polycondensation of $Ga(OH)_3$ to α-GaOOH rods, which possess a hierarchical layered nanostructure coated by SF peptide chains. The α-Ga_2O_3 and β-Ga_2O_3 rods can be obtained by thermal treatment of the α-GaOOH rods at 600 and 800 °C, respectively. The morphological characteristics of the α-GaOOH rods are well-maintained in the oxide products in terms of good dispersion, size uniformity, and layered nanostructure. These as-prepared gallium oxide rods, especially the β-Ga_2O_3 rod, present a strong blue luminescence emission in the excitation wavelength of 276 nm. It is believed that the method can be used to synthesize other excellent optical metal and semiconductor oxide micrometer

(51) Lovric, J.; Cho, S. J.; Winnik, F. M.; Maysinger, D. *Chem. Biol.* **2005**, *12*, 227.
(52) Xia, T.; Kovochichi, M.; Brant, J; Hotze, M.; Sempf, J.; Oberley, T.; Sioutas, C.; Yeh, J. I. *Nano Lett.* **2006**, *6*, 1794.
(53) Green, M.; Howman, E. *Chem. Commun.* **2005**, *1*, 121.
(54) Chiarini, A.; Petrini, P.; Bozzini, S.; Pra, I. D.; Armato, U. *Biomaterial* **2003**, *24*, 789.
(55) Minoura, N.; Aiba, S.; Higuchi, M.; Gotoh, Y.; Tsukada, M.; Imai, Y. *Biochem. Biophys. Res. Commun.* **1995**, *208*, 511.

rods since the synthesis procedure is relatively simple. Toxicological impact studies of gallium oxide rods upon L929, Hela, and HaCat cell lines presented excellent cellular compatibility, suggesting their possible application in bio-optoelectronic devices in the future.

Acknowledgment. This work has been supported by the National Natural Science Foundation of China (project nos. 60871062 and 50873066). The support of Sichuan Province through a Science Fund for Distinguished Young Scholars of Sichuan Province (08ZQ026-007) and Key Technologies Research and Development Program of Sichuan Province (2008SZ0021 and 2006Z08-001-1) are also acknowledged with gratitude. This work was also supported by the *Research Fund for the Doctoral Program of Higher Education from Ministry of Education of China* (No. 20070610131). We thank Analytical & Testing Center, Sichuan University, for the assistance with the microscopy and XRD work.